ELSEVIER

Journal of Power Sources 75 (1998) 283–287

JOURNAL OF POWER SOURCES

Short communication

# Electrochemical behaviour of $Ni(OH)_2$ ultrafine powder

Yunshi Zhang, Zhen Zhou, Jie Yan *

*Institute of New Energy Material Chemistry, Nankai University, Tianjin 300071, China*

Received 8 May 1998; accepted 13 May 1998

**Abstract**

Ultrafine $Ni(OH)_2$ powder is prepared by converting a $Ni_2C_2O_4$ precipitate in NaOH solution which contained Tween-80. The sample prepared by this method is β(II)-type phase and its particle size is about 30 nm. The electrochemical behaviour of nickel foam electrodes using this ultrafine $Ni(OH)_2$ powder as active material is studied and compared with micron-sized spherical $Ni(OH)_2$ by means of a galvanostatic charge–discharge method, cyclic voltamperommetry (CV) and electrochemical impedance spectroscopy (EIS). It is found that ultrafine $Ni(OH)_2$ powder has superior electrochemical properties, such as lower polarization, better reversibility, and smaller reaction resistance. 

*Keywords:* Nickel hydroxide; Ultrafine powder; Preparation; CV; EIS

## 1. Introduction

Secondary alkaline batteries, such as nickel/cadmium and nickel/metal hydrides cells, have been developing quickly in recent years. In order to improve the performance of these batteries, paste-type $Ni(OH)_2$ electrodes have been widely employed [1,2]. This type of nickel electrode is prepared by incorporating paste-type $Ni(OH)_2$ as an active material in a nickel foam or fibre substrate. The $Ni(OH)_2$ used most widely in paste-type electrodes is the spherical variety, which is prepared by chemical precipitation [3–5] before electrode preparation. Watanabe and Kikuoka [2] have studied the electrochemical characteristics of spherical $Ni(OH)_2$ and have found that $Ni(OH)_2$ with a smaller crystalline size displays better electrochemical properties.

The spherical $Ni(OH)_2$ used in paste-type nickel electrodes usually has a particle diameter from several microns to tens of microns. In fact, the electrochemical properties of micron-sized spherical $Ni(OH)_2$ are not so good, i.e., the discharge capacity, electric conductivity and proton diffusion ability are quite low. On the other hand, because spherical $Ni(OH)_2$ has a higher taping density and can be more easily introduced into nickel substrates, it is used widely in paste-type nickel electrodes.

In this paper, ultrafine $Ni(OH)_2$ powder (UFP) is prepared by a so-called precipitate-transformation method [6]. The aim is to compare the electrochemical behaviour of the $Ni(OH)_2$ UFP with that of micron-sized spherical $Ni(OH)_2$ which is used widely in paste-type nickel electrodes.

## 2. Experimental

### 2.1. Preparation and characterization of $Ni(OH)_2$ UFP

The synthesis of $Ni(OH)_2$ UFP was made as follows. Solutions of 0.2 M $NiSO_4$ and 0.2 M $Na_2C_2O_4$ were mixed and stirred constantly to yield a precipitate of $NiC_2O_4 2H_2O$. The $NiC_2O_4 2H_2O$ precipitate was converted to a $Ni(OH)_2$ precipitate in NaOH solution which contained a small amount of Tween-80. The reaction system was kept at 60°C and stirred constantly for 1 h. The Tween-80 was used to prevent the newly produced $Ni(OH)_2$ crystals from growing and aggregating. Finally, the $Ni(OH)_2$ precipitate was filtered, rinsed with distilled water, and oven-dried at 60°C.

The XRD pattern for the prepared powder was obtained with a Rigaku D/max-IIIA diffractometer using CuKα radiation and a graphite filter at 40 kV and 50 mA. Transmission electron microscopic (TEM) studies were performed using a Hitachi H-800 microscope. Before observation, the sample was ultrasonically dispersed in ethanol. The surface areas of different $Ni(OH)_2$ samples

* Corresponding author. Tel.: +86-22-2350-26-04; Fax: +86-22-2350-26-04; E-mail: zhangys@sun.nankai.edu.cn

0378-7753/98/$19.00 
PII: S0378-7753(98)00111-6

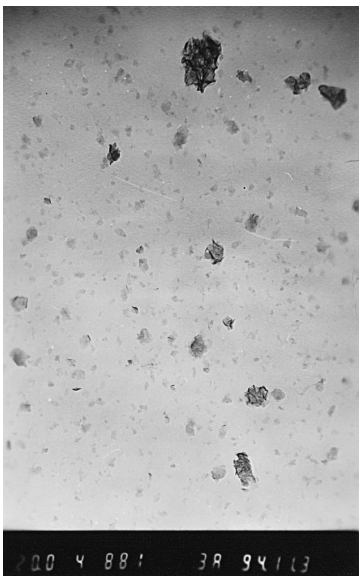

Fig. 1. TEM photograph of $Ni(OH)_2$ UFP ($\times 10^5$).

were obtained by the BET adsorption method using a surface area analyzer.

### 2.2. Preparation of nickel electrodes

The $Ni(OH)_2$ UFP (or the micron-sized spherical $Ni(OH)_2$ powder) was mixed with an adequate amount of distilled water to obtain a paste mixture. The mixture was incorporated in the centre of a $1 \times 1$ $cm^2$ nickel foam using a spatula and a second layer of nickel foam was applied under pressure to prevent shedding of the $Ni(OH)_2$ powder since no binder was used. The resulting electrodes were dried in air at room temperature and pressed at 20 MPa. Finally, nickel ribbon current-collectors were spot-welded to the electrodes.

### 2.3. Electrochemical measurements

Charge–discharge measurements of the nickel electrodes were performed using a glass beaker cell. A hydrogen-storage alloy electrode with an excessive capacity was used as the counter electrode, and 6 M KOH was used as the electrolyte. A Hg/HgO (6 M KOH) electrode was employed as the reference electrode. Charging was carried out at the 0.2 C rate for 7.5 h. After a rest of 30 min,

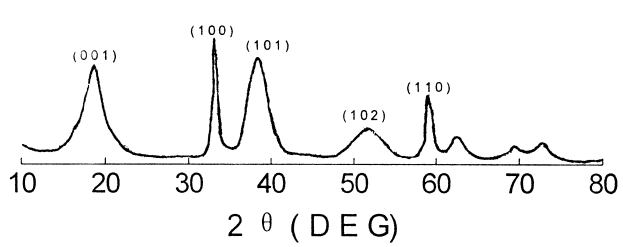


Fig. 2. XRD pattern of $Ni(OH)_2$ UFP.

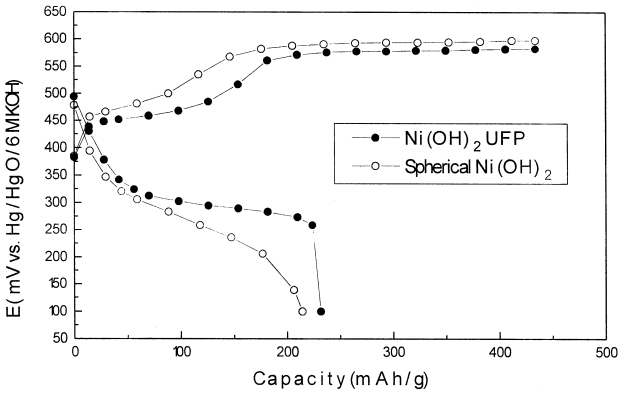


Fig. 3. Charge–discharge curves of different samples of $Ni(OH)_2$.

discharging was conducted at the same rate down to 0.1 V vs. Hg/HgO electrode. All tests were performed at room temperature.

Cyclic voltammetric (CV) experiments were performed by means of a TD 3690 potentiostat, controlled by an external computer, and a three-electrode system with a Hg/HgO reference electrode and a hydrogen-storage alloy counter electrode with a large area.

Electrochemical impedance spectra (EIS) were obtained at open-circuit using a solartron 1250 frequency analyzer in combination with a computer. The impedance spectra of the electrodes were recorded from 10 kHz to 10 mHz and at 5 mV amplitude of perturbation. The impedance spectra were fitted to an equivalent circuit using a nonlinear, least squares (NLLS) fitting program EQUIVCRT [7].

## 3. Results and discussion

### 3.1. Characterization of $Ni(OH)_2$ UFP

The $Ni(OH)_2$ UFP, prepared by a precipitate-transformation method, consisted of thin, single particles of about

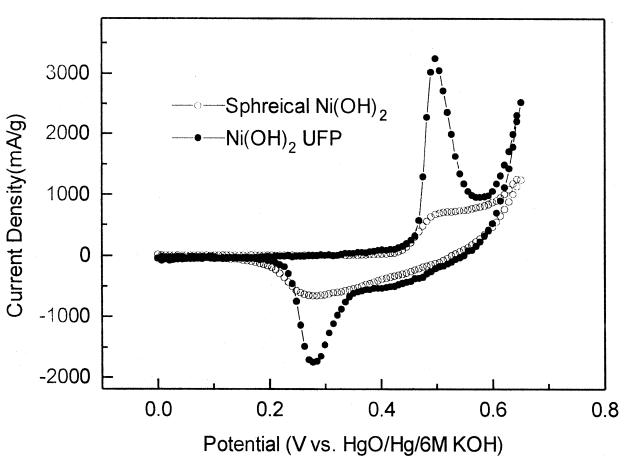


Fig. 4. Cyclic voltammograms of different samples of $Ni(OH)_2$ before activation; scan rate: 1 mV $s^{-1}$.

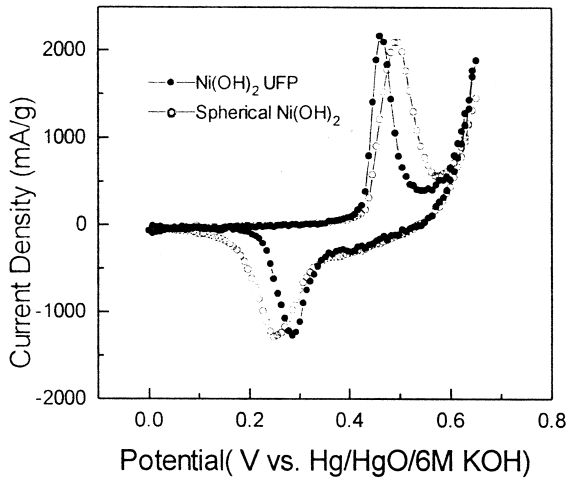


Fig. 5. Cyclic voltammograms of different samples of $Ni(OH)_2$ after three-cycle activation; scan rate: 0.5 mV $s^{-1}$.

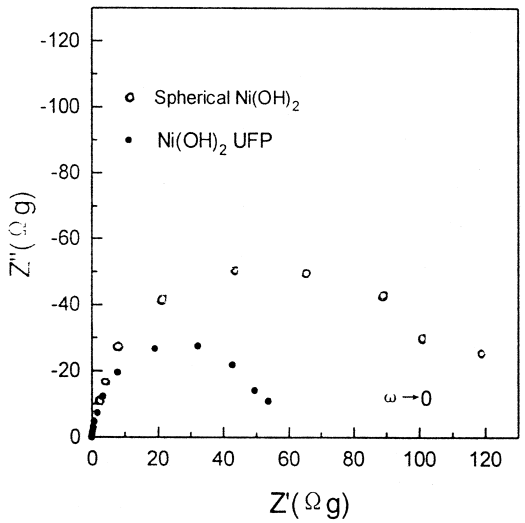


Fig. 6. Complex plane plots for different samples of $Ni(OH)_2$ before activation.

30-nm average diameter, as seen by TEM (Fig. 1). The XRD pattern of this sample is given in Fig. 2 and shows that the prepared sample is typically β(II)-type $Ni(OH)_2$ phase. The crystal size of the $Ni(OH)_2$ UFP was also estimated by Scherrer formula [8] because all its XRD peaks were broadened. The crystal size is, respectively, 2 nm and 20 nm as calculated from the (100) and the (101) crystal face. The spherical $Ni(OH)_2$ used in the experiments is also β(II) phase, and its average particle size is about 20 μm. The BET surface areas of spherical $Ni(OH)_2$ and $Ni(OH)_2$ UFP are 9.9 and 36.5 $m^2$ $g^{-1}$, respectively.

### 3.2. Galvanostatic charge–discharge experiments

Nickel electrodes using $Ni(OH)_2$ were galvanostatically charged and discharged at the 0.2 C rate. Typical charge–discharge curves are presented in Fig. 3. It can be seen that the charging potentials of $Ni(OH)_2$ UFP are lower than those of spherical $Ni(OH)_2$, but the discharging potentials of $Ni(OH)_2$ UFP are higher in comparison. There are two charging plateaux in both charging curves. It is suggested that the lower plateaux correspond to the reaction: $Ni(OH)_2 + OH^- \rightarrow NiOOH + H_2O + e^-$, while the other

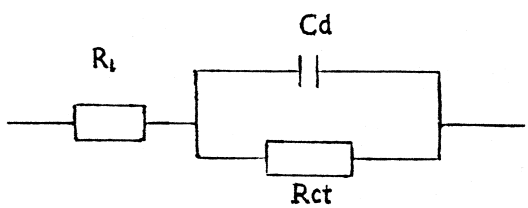


Fig. 7. Equivalent circuit for $Ni(OH)_2$ electrodes.

plateaux correspond to oxygen evolution. Since the plateau of $Ni(OH)_2$ UFP oxidation is longer than that for spherical $Ni(OH)_2$, the former material can be oxidized more completely during the charging process. The discharging plateau of $Ni(OH)_2$ UFP is higher and more level than that of spherical $Ni(OH)_2$. Moreover, the discharging capacity per gram of $Ni(OH)_2$ UFP is greater than that per gram of spherical $Ni(OH)_2$, viz., 232 vs. 214 mAh $g^{-1}$. Given these findings, it can be concluded that $Ni(OH)_2$ UFP experiences less polarization during electrochemical reaction, which should be demonstrated more clearly in the following CV and EIS results.

Table 1
Experimental data from cyclic voltammetric measurements

| Electrode | Before activation | | After activation | |
|---|---|---|---|---|
| | Spherical $Ni(OH)_2$ | $Ni(OH)_2$ UFP | Spherical $Ni(OH)_2$ | $Ni(OH)_2$ UFP |
| $E_{p,a}$ (V) | 0.507 | 0.496 | 0.493 | 0.456 |
| $E_{p,c}$ (V) | 0.274 | 0.280 | 0.244 | 0.286 |
| $\Delta E_{pa,c}$ (V) | 0.233 | 0.216 | 0.249 | 0.170 |

$E_{p,a}$ denotes anodic potential.
$E_{p,c}$ denotes cathodic potential.
$\Delta E_{pa,c}$ denotes the differences in the former two potentials.

Table 2
Charge-transfer resistance, $R_{ct}$, of different samples of $Ni(OH)_2$ samples

| Electrode | Before activation | | After activation | |
|---|---|---|---|---|
| | Spherical $Ni(OH)_2$ | $Ni(OH)_2$ UFP | Spherical $Ni(OH)_2$ | $Ni(OH)_2$ UFP |
| $R_{ct}$ ($\Omega$ g) | 98.33 | 56.38 | 4.245 | 3.344 |

### 3.3. Cyclic voltammetric measurements

Cyclic voltammetric measurements were made on nickel foam electrodes using $Ni(OH)_2$ UFP or spherical $Ni(OH)_2$ as the active material. The cyclic voltammograms of these two electrodes before activation are given in Fig. 4, and the voltammograms after three charge–discharge cycles are shown in Fig. 5. The data in Figs. 4 and 5 are listed in Table 1 in more detail. It should be noted that the current units in CVs were normalized to the weight of the active materials, since it was difficult to estimate the real surface area of the porous nickel foam substrate [9]. The same procedure was used in the following EIS experiments.

It can be seen from Fig. 4 that, before activation, the cathodic and the anodic peak current densities of $Ni(OH)_2$ UFP are much higher than those of spherical $Ni(OH)_2$. This indicates that $Ni(OH)_2$ has a much higher electrochemical reactivity and a faster activation. After three charge–discharge cycles, the peak current densities of spherical $Ni(OH)_2$ are close to those of $Ni(OH)_2$ UFP, see Fig. 5. It can also be deduced from Figs. 4 and 5, and more clearly in Table 1, that, both before activation and after three charge–discharge cycles, the anodic peak potentials of $Ni(OH)_2$ UFP are lower than those of spherical $Ni(OH)_2$, and the cathodic peak potentials of $Ni(OH)_2$ UFP are higher than those of spherical $Ni(OH)_2$. This observation is in good agreement with the above charge–discharge experimental results, which also indicates that an electrode using $Ni(OH)_2$ UFP as active material has smaller polarization during the electrochemical redox process. In order to compare the characteristics of electrodes, the difference in the anodic and cathodic peak potentials, $\Delta E_{pa,c}$, was taken as an estimate of the reversibility of the redox reaction [10,11]. The resulting data are also listed in Table 1, and show that the $\Delta E_{pa,c}$ of $Ni(OH)_2$ UFP is much smaller than that of spherical $Ni(OH)_2$, either before or after activation. Thus, the $Ni(OH)_2$ UFP electrode has better redox reversibility.

### 3.4. Electrochemical impedance spectra

Impedance measurements provide a promising method for the study of the characteristics of electrochemical reaction systems. There have been many studies [12–15] of the impedance of nickel electrodes. Complex plane plots for nonactivated electrodes using $Ni(OH)_2$ UFP or spherical $Ni(OH)_2$ as active material are shown in Fig. 6. The impedance spectra for these two electrodes display an obvious semicircle and no slope related to the Warburg impedance appears in the high-frequency region. Since no additives and conductive agents were added during the processes of the electrode preparation and the active material synthesis, it is difficult for the electrochemical reaction to proceed and the charge-transfer resistance is very large; therefore, the impedance spectra only show an arc of capacitive reactance. An NLLS fitting calculation was performed using the equivalent circuit shown in Fig. 7. The equivalent circuit for electrode consists of the following components: the electrolyte resistance, $R_1$; the charge-transfer resistance, $R_{ct}$; the double-layer capacitance $C_d$. The experimental curves in the complex plane plots can be fitted very satisfactorily by a semicircle, and values of $R_{ct}$, which can be used to estimate the characteristics of electrodes, are listed in Table 2 including those for electrodes before and after activation. It is found that the charge-transfer resistance, $R_{ct}$, of the $Ni(OH)_2$ UFP before activation is much smaller than that of spherical $Ni(OH)_2$, but after a three-cycle activation, the two values are much closer. This indicates that the electrochemical reaction of $Ni(OH)_2$ UFP proceeds more easily than that of spherical $Ni(OH)_2$.

$Ni(OH)_2$ UFP synthesized by this method has a very small crystal size and a large surface area. Thus, contact between the active material and the electrolyte is enhanced. Moreover, the distance for proton diffusion in the crystal lattice is shortened. Accordingly, the superior electrochemical performance of $Ni(OH)_2$ UFP is readily understood.

## 4. Conclusions

$Ni(OH)_2$ UFP prepared by the precipitate-transformation method can serve as the active material for nickel electrodes. Characterization by XRD and TEM shows that it has a typical $\beta$(II)-phase structure and a particle size of about 30 nm.

Electrochemical measurements reveal that the performance of $Ni(OH)_2$ UFP is superior to that of micron-sized spherical $Ni(OH)_2$, e.g., it has better reversibility, lower polarization, smaller charge-transfer resistance, and faster activation.

## References

[1] M. Oshitani, H. Yufu, K. Tskashima, Y. Matsumara, J. Electrochem. Soc. 136 (1989) 1590.
[2] K. Watanabe, T. Kikuoka, J. Appl. Electrochem. 25 (1995) 219.
[3] Matsushita Electric Industrial, JP 60, 131 (1985) 765.
[4] M. Honda, T. Minora, JP 03, 252 (1991) 318.
[5] T. Minora, JP 02, 06 (1990) 340.
[6] G.-T. Zhou, S.-H. Liu, Y.-F. Zheng, Chinese Science Bulletin 41 (1996) 321, in Chinese.
[7] B.A. Boukmap, Solid State Ionics 20 (1986) 31.
[8] B.D. Cullity, Elements of X-ray Diffraction, 2nd edn., Addison-Wesley Publishing, 1978, p. 102.
[9] M.J. Avena, M.V. Vazquez, R.E. Carbonio, C.P. De Pauli, V.A. Macagno, J. Appl. Electrochem. 24 (1994) 256.
[10] P.V. Kamath, M.F. Ahmed, J. Appl. Electrochem. 23 (1993) 225.
[11] D.A. Corrigan, R.M. Bendert, J. Electrochem. Soc. 136 (1989) 723.
[12] S. Passerini, B. Scrosati, J. Electrochem. Soc. 141 (1994) 889.
[13] M.A. Reid, P.L. Loysell, J. Power Sources 36 (1991) 285.
[14] K.A. Murugesamoorthi, S. Srinivasan, A.J. Appleby, J. Appl. Electrochem. 21 (1991) 95.
[15] S. Kulcsar, P. Horvath, G. Csath, M. Smaroglay, J. Power Sources 8 (1982) 61.